Low-temperature homoepitaxial growth on nonplanar Si substrates

D. P. Adams and S. M. Yalisove
Department of Materials Science and Engineering, University of Michigan, 2300 Hayward Street, Ann Arbor, Michigan 48109-2136

(Received 27 April 1994; accepted for publication 21 July 1994)

The kinetics associated with the breakdown of epitaxy at low temperatures are studied for growth onto a number of Si surfaces, including (001), (117), (115), and (113). These surfaces are all initially generated at trench edges on a single patterned substrate. Growth on each of these surfaces at low temperatures is shown to result in a well-defined crystalline-to-amorphous transition. The epitaxial thicknesses h_{epi} have been measured over a range of substrate temperatures below 280 °C, and activation energies characteristic of this transition were determined. In general, the breakdown in epitaxy occurs such that $h_{epi}(001)>h_{epi}(117)>h_{epi}(115)>h_{epi}(113)$. Growth at slightly higher temperatures, $T_{substrate}>300$ °C, shows a different microstructure than that at lower temperatures. Epitaxial growth continues for longer times on (113) facets, as compared with (001). These results are discussed in terms of a recently proposed model explaining the breakdown of epitaxy at lower temperatures and an epitaxial temperature for Si.

I. INTRODUCTION

Thin film growth onto nonplanar substrates is currently an integral part of the fabrication of electronic devices and the construction of structures such as quantum wires and dots.[1–3] In general, patterned substrates are useful for outlining or defining areas for layer growth in very large scale integration. However, applications requiring submicron minimum feature sizes have now begun to use novel patterned structures which consume less wafer area. This is accomplished by building layers out of the wafer plane,[4–6] using structures such as V grooves. These designs often take advantage of the fact that growth onto nonplanar substrates results in the formation of well-defined facets at a trench edge,[7–14] typically along high Miller index surfaces, such as (113).

In this investigation, the facets created at a trench edge during a high-temperature step are not the primary subject of this work but are used instead as starting surfaces to monitor subsequent low-temperature molecular-beam-epitaxial (MBE) growth.[15–17] The impetus for this study of growth onto nonplanar substrates is to provide a better understanding of a recently discovered epitaxial thickness phenomenon.[18] In that work, Eaglesham and co-workers have shown that a breakdown in homoepitaxy occurs during growth on Si(001) at low temperatures.[18] Si layers deposited at temperatures below ~450 °C were found to initially develop as single-crystalline material but then turn amorphous at a critical thickness, designated h_{epi}.[18,19] The discovery of an epitaxial thickness has a strong impact on our understanding of thin-film growth, for it demonstrates that epitaxial growth [at least for Si deposited onto Si(001)] does not follow the classic description, involving only a critical temperature.[20,21]

Since the discovery of an epitaxial thickness, a number of key observations related to this breakdown in single-crystal growth have been made. Several groups have demonstrated that this transition is intrinsic to low-temperature growth and is not an effect of impurities (e.g., hydrogen).[19,22,23] Growth of Si under clean, ultrahigh-vacuum (UHV) conditions does exhibit a crystalline-to-amorphous transition and is characterized by an epitaxial height which depends on substrate temperature (Arrhenius relation).[18] It is noted that while impurities are not responsible for the breakdown in epitaxy, h_{epi} is very sensitive to small amounts of H.[19,24] More recently, roughening that occurs during the epitaxial portion of the film's history was identified as a cause of the transition to an amorphous state.[22] It was also shown in that work that the effect of H, when introduced during growth, is to increase the roughening rate, thereby lowering h_{epi}. However, despite much progress, additional work is still needed to identify the role of islanding and other processes that could be influencing a breakdown in crystallinity during homoepitaxial growth.

This study focuses on the mechanisms underlying the crystalline-to-amorphous transition, by monitoring the changes in microstructure that occur during growth on a number of different Si surfaces. It is found that low-temperature Si homoepitaxial growth on several surfaces, other than (001) and (111),[25] does result in a crystalline-to-amorphous transition. Furthermore, by monitoring h_{epi} over a range of temperatures, an accurate comparison of the "activation energies" characteristic of this transition has been made. Nonplanar substrates have been useful for probing this breakdown in epitaxy, for several surfaces are contained on a single substrate. In this way, large errors in temperature reproducibility, which inevitably occur when using multiple substrates, are avoided. It is noted that while much is already known about the growth kinetics on reconstructed Si(001) surfaces,[26] little effort has been devoted toward understanding growth on other high-index Si surfaces.

II. EXPERIMENT

The Si⟨001⟩ wafers used for testing were p type with 0.20–0.40 Ω cm resistivity. These were initially patterned using conventional UV lithography and plasma etching into structures described elsewhere as corrugated substrates[27] or mesa stripes. On each 3 in. wafer, trenches were aligned in the ⟨110⟩ direction (±0.5°), extending across the entire sur-

 0021-8979/94/76(9)/5185/5/$6.00 © 1994 American Institute of Physics

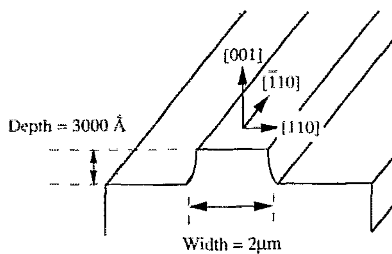

FIG. 1. Schematic of patterned Si substrates.

face with a depth of 3000 Å and a wavelength of 4 μm (see Fig. 1). Wafers were cleaned after etching by stripping photoresist from the surface. Wafers were then diced into rectangular samples and further cleaned using a modified RCA procedure.[28] A protective oxide was chemically grown as a last step in this cleaning process. Si substrates were then loaded onto sample holders between Ta clips, also used for passing direct current through the Si for heating. For each deposition, samples were mounted such that the trenches were parallel to the direction of current flow.

Sample holders were placed into an ultra-high-vacuum (UHV) MBE system (base pressures: 7×10^{-11} Torr) via a load-lock chamber.[29] Each sample was then outgassed in a separate preparation chamber at 200 °C for 30 min, 400 °C for 30 min, and 600 °C for 1 h.[30] After entry into the growth and analysis chamber, the protective oxide was removed by heating to 950 °C for 1 min, and low-energy electron diffraction and Auger electron spectroscopy were used to ensure that a clean, reconstructed surface was obtained. MBE growth of ~500-Å-thick undoped Si buffer layers at 600 °C (0.2 Å/s) was used to bury the residual contamination on all portions of nonplanar substrates. Samples were then quenched, equilibrated for 15 min at a particular low growth temperature, and coated with 1 monolayer of Ge in order to accurately mark the start of low temperature growth. Low-temperature Si homoepitaxial growth involved deposition at a rate of 0.16 Å/s [calibrated for the (001) terrace], while keeping the substrate maintained at a fixed temperature between 70 and 400 °C.[31]

It was found that the surface profile of Si buffer layers (i.e., the starting structure for low-temperature growth) in each sample was dominated by (113) facets at the trench edge.[9] Also, additional well-developed high-index facets [namely (115) and (117)] were developed during buffer layer growth at 600 °C, although only at the bottom of the mesa stripe. These (115) and (117) facets did make up a smaller fraction of the step-edge profile, when compared to the length of the (113) facets. Nevertheless, the facets were of sufficient length to accurately monitor low-temperature growth on the particular surface. The Si arrival rates for the other facet surfaces are calculated by their angular deviation from the (001) surface (i.e., projected area). Based on the 0.16 Å/s rate set for the (001) terrace, these are 0.14 Å/s for the (113) facet, 0.15 Å/s for the (115) facet, and ~0.16 Å/s for (117). Note, in our chamber apparatus, that the substrates are fixed at a distance of 22 in. from the Si gun, with a flux incidence angle of approximately 4° relative to the wafer normal direction.

Transmission electron microscopy (TEM) was used to monitor the changes in microstructure that developed during low-temperature growth. Cross-section TEM samples were prepared by mechanically thinning to 50 μm, followed by ion milling until perforation. In this study, the epitaxial thickness for each surface has been measured in the direction normal to the particular facet plane. This height, referred to as $h_{epi}(hkl)$, was taken to be the thickness at which one-half the layer turned amorphous, as in the original definition.[18] Average values of h_{epi} were measured from areas in the middle of each facet, i.e., away from the intersection points of adjacent facets. This was also done on the (001) surfaces, in order to avoid any effect that a facet-facet intersection point might play on growth. In addition, control experiments consisting of depositing a Ge marker layer over only half of the sample showed that the marker layers did not change the epitaxial thickness. Also no difference in epitaxial thickness was found for growth on the two opposite sides of a single trench.

III. RESULTS

The changes in microstructure that are typical for growth at temperatures below ~300 °C are shown in two cross-section TEM micrographs, Figs. 2 and 3. Figure 2 shows a cross-section view of a Si layer grown at 190 °C onto a thick buffer layer. In this sample, it can be seen that epitaxial growth on the Si(001) surface continues for a greater time than on Si(113). A smooth transition from crystalline to amorphous material is exhibited on both surfaces, after approximately 265 Å on the Si(001) surface and at 110 Å on Si(113). Figure 3 shows a cross-section TEM image of a layer also deposited at 190 °C. The area from which this image was taken is located at the bottom of a trench edge, where the surface profile is multifacetted. Here the (111), (113), (115), and (117) Si starting surfaces, used for low-temperature growth, are shown by a Ge marker layer, seen as

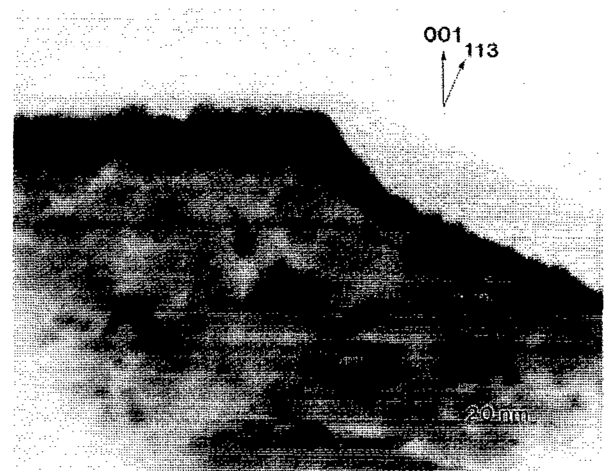

FIG. 2. Cross-section TEM image of a Si layer deposited on patterned Si(100) after buffer layer growth. Low-temperature growth of Si was conducted at $T_{substrate}=190$ °C, beginning at the Ge marker shown.

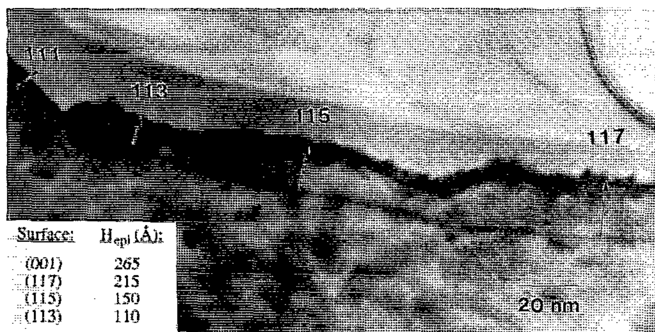

FIG. 3. TEM micrograph of Si layer grown at 190 °C onto a multifaceted wafer. H_{epi} for the different surfaces present on this sample [including (001)] are listed in the bottom left-hand-side corner.

a thin dark line. Low-temperature growth onto each of these surfaces is found to result in a breakdown in epitaxy. A well-defined crystalline-to-amorphous transition occurs on the (113), (115), and (117) surfaces, while almost no epitaxial growth has occurred on the (111) facet. (Arrows are used to mark the epitaxial thicknesses for the various surfaces, with values of h_{epi} listed in the bottom left-hand-side corner.) The epitaxial thicknesses resulting from growth over a range of substrate temperatures, up to 280 °C, are shown in Fig. 4 where epitaxial height is plotted against $1/T$ (K). Activation energies characteristic of this transition have also been extracted, by assuming an Arrhenius fit to these curves, as in a previous study.[18]

Surprisingly, Si layers exhibit a markedly different microstructure when grown at slightly higher temperatures. This difference is seen clearly in Fig. 5 for a layer grown at $T_{substrate}$=325 °C. In this sample, epitaxial growth along the Si(113) surface continued for much greater time than would be predicted using the data in Fig. 4. Extrapolation of the curve in Fig. 4 describing Si(113) predicts that $h_{epi}(113)$ should be ~450 Å at this temperature; however, epitaxial growth on the Si(113) facet has continued for the entire 2000 Å layer thickness. On the other hand, epitaxial growth on the Si(001) portion of the same nonplanar substrate is consistent with the data found at lower temperatures. Even though this layer was not grown to a thickness equal to $h_{epi}(001)$, early

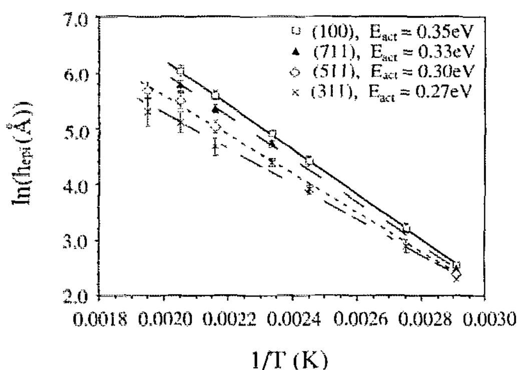

FIG. 4. Plot of ln(h_{epi}) vs 1/temperature for four different Si surfaces.

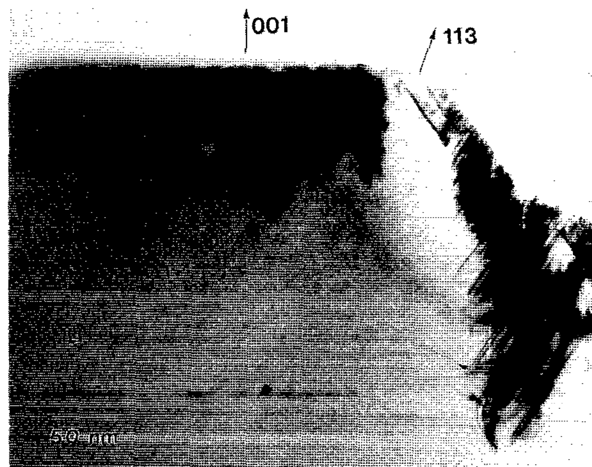

FIG. 5. Cross-section TEM image of Si layer grown onto a patterned Si(001) wafer at $T_{substrate}$=325 °C. Ge marker layer is identified with arrowheads. Note: The large number of stacking faults to the right-hand side of the (113) facet arises from low-temperature growth onto a neighboring {111} facet.

evidence of a transition to a highly disordered state (in the form of stacking faults and polycrystalline material)[32] is seen at a thickness of 1500 Å.

IV. DISCUSSION

This work demonstrates that the breakdown of epitaxial growth at low temperatures is strongly influenced by the starting surface. In particular, the crystalline-to-amorphous transition is found in this study to occur on several high-index Si surfaces, in addition to growth on Si(001).[33,34] Figure 3 shows the differences in microstructure that develop for simultaneous growth on (113), (115), and (117) Si surfaces. A comparison of the kinetics responsible for the breakdown of epitaxy from surface to surface has been made by measuring h_{epi} over a range of temperatures. This comparison of the kinetics is accurate, because each of the surfaces was contained on the same substrate and the temperatures were the same. The fits to the curves in Fig. 4 show an epitaxial height dependence on substrate temperature (in a regime where $T_{substrate}$<280 °C) that closely follows an Arrhenius relation. The activation energies characteristic of the transition E_{act} were determined to be 0.35, 0.33, 0.30, and 0.27 eV for the (001), (117), (115), and (113) Si surfaces, respectively. It is noted that the value of E_{act} for growth on the (001) surface is in agreement with previous work involving growth onto flat Si(001) substrates. That work has shown that $E_{act}(001)$ is 0.4 eV.[35]

The question then arises: Why is h_{epi} lower for growth on high Miller index surfaces? In order to answer this question, one needs an understanding of the kinetics for growth on each of the surfaces. The explanation for why

$$h_{epi}(001)>h_{epi}(117)>h_{epi}(115)>h_{epi}(113)$$

for substrate temperatures below ~300 °C is suggested here to be related to the initial surface roughness of each of the surfaces. This would not be surprising considering that an increase in surface roughness has been strongly correlated

with the breakdown of epitaxy on Si(001).[22] In addition, this previous work showed that areas on Si(001) wafers having a large, initial surface roughness exhibited a premature breakdown in epitaxy (compared with growth on smooth regions on the same substrate).[22] For growth onto the high-index Si surfaces, a large initial surface roughness would then be expected to affect layer growth, perhaps by limiting Si adatom migration lengths.

While little is known about the kinetics of adatom motion on these high Miller index surfaces, there has been a large amount of work devoted toward characterization of their stable surface structure. After reviewing the literature, we find that the (117), (115), and (113) surfaces established during buffer layer growth are likely to be "rougher" than the dimerized Si(001) surface. The simplest description of these three surfaces considers each as being vicinal to the (001). In that scenario, the terrace widths are smaller ($\sim$1 or 2 ⟨110⟩ spacings) for larger angles of miscut. This may be an accurate description of the (117) surface, for it has been shown to have a very large density of small (001) terraces[36] (see Chadi for why this may not be true[37]). However, the same description [i.e., as surfaces made up of (001) terraces] is not accurate for Si(113) and Si(115). A number of works have demonstrated that the Si(113) and Si(115) surfaces are both reconstructed. The Si(113) surface is thought to reconstruct with either a (1×3) or a (2×3) structure,[38–41] while the Si(115) surface is believed to reconstruct with a (1×3) surface cell.[36] At least one of the high-index surfaces has been found to contain a large number of domain boundaries with areas of different reconstruction forming in close proximity. For example, Knall *et al.* has recently shown that the (113) surface exclusively has a (3×2) rearrangement and explains the observations of a (3×1) low-energy electron-diffraction pattern in terms of isolated domains of (3×2) reconstructed Si.[41] Also, we expect that microfacets (of other orientation) may be present on the starting surfaces or develop during low temperature homoepitaxial growth. In either of these cases, the initial surface topography of the high Miller index surfaces,[40,42,43] or more specifically the paths over which diffusing atoms travel during layer growth, is expected to be different than that of dimerized Si(001).

Two additional points must be noted. An assumption has been made in the interpretation of growth kinetics for the different facets compared to that of Si(001). This work considers the surface roughness on the (001) portions of nonplanar substrates to initially be small. Recent work by Hirayama, Hiroi, and Ide studying Si selective epitaxial growth onto SiO_2 patterned surfaces has shown that this is most likely the case.[44] That work demonstrated that flat (001) mesa tops always result from growth at higher temperatures, independent of the step density on the (001) surface (initial miscuts as large as 4° were tested). TEM analysis in this study using Ge marker layers has indicated that a smooth Si(001) starting surface is created during buffer layer growth. Another point that is critical to this analysis involves the differences in Si flux arriving at the Si facets. The small change in deposition rate for the different surfaces ($\sim$0.02 Å/s) set by the geometry of the substrate is not thought to affect h_{epi}. This is because a variation in deposition rate (over orders of magnitude, from 50 to 0.5 Å/s) has been shown to have no effect on h_{epi} for Si(001).[19] We assume that this is true also for growth on other $\{hkl\}$ surfaces. Furthermore, the effects of shadowing may also be important. It is thought that shadowing[45] of incoming Si atoms by asperities on the surface certainly could influence the kinetics in this experiment, since roughening is known to occur during low-temperature growth. In this way, the (113) facet would be affected most, because it is the steepest surface studied. It is noted that at this time little is known about the influence of deposition angle on the epitaxial thickness. Nevertheless, both explanations of reduced h_{epi} on the facets (i.e., as due to the initial roughness of the particular facet or as due to shadowing) indicate that surface roughening is intrinsically involved with the breakdown. A systematic study of growth onto tilted Si(100) substrates should reveal whether an oblique deposition geometry has any effect.

Given the model for explaining the trends in h_{epi} based on surface disorder, it is interesting that extrapolation of the curves shown in Fig. 4 does not accurately describe growth at higher substrate temperatures on Si(113) but does correctly predict $h_{epi}(001)$. We consider one likely explanation for this behavior. A justification for a larger epitaxial thickness on certain facets, such as (113), could involve description of single-crystal growth by use of an epitaxial temperature, T_{epi}. Although earlier work demonstrated that an epitaxial thickness must be included in the full description of low-temperature Si homoepitaxy,[18] an epitaxial temperature may also exist. The difference in microstructure between that indicated in Fig. 4 and the micrograph in Fig. 5 could then be explained if the epitaxial temperature depends on the growth surface [i.e., $T_{epi}(113)<T_{epi}(001)$]. (This description should also include discussion of any change in surface lattice reconstruction that might occur at a higher temperature.) However, in order to correctly interpret these data one may need to consider the role of the nonplanar substrate geometry on growth. In particular, for growth at higher temperatures it is thought that the (113)-(001) facet intersection "point" could also be affecting the resultant growth morphology. It has been suggested in other work on GaAs that atoms landing on a sidewall facet do tend to migrate toward the neighboring (001) surface during growth at higher temperatures.[10] In fact for Si layer growth, preferential relocation of adatoms on the (001) surface has been shown to continue until the top of the mesa structure is pinched off [i.e., with (113) facets extended to the top of the stripe].[44] The mechanisms underlying this effect may also be influencing epitaxial growth of Si on sidewall facets at 325 °C. Of course, the effects of kinetics and energetics[46] must be distinguished in order to identify why formation along (113) is preferred.

V. CONCLUSIONS

This study demonstrates the changes in microstructure which can develop on different Si surfaces. The (113), (115), and (117) Si surfaces have now been shown to exhibit a well-defined crystalline-to-amorphous transition, previously found to occur on (001) substrates. Using nonplanar substrates, the activation energies characteristic of this transition have been determined to be 0.35 ± 0.05, 0.33 ± 0.05, 0.30

±0.05, and 0.27±0.05 eV for the (001), (117), (115), and (113) Si surfaces, respectively. The differences in h_{epi} found to occur for a given substrate temperatures below 300 °C are explained by a model in which a large initial surface roughness (perhaps influenced by shadowing) leads to the formation of amorphous material at smaller layer thicknesses. It is noted here that growth at a slightly higher temperature, 325 °C, does not agree with the trends found at lower temperatures; however, we believe that the epitaxial thicknesses reported in Fig. 4 are characteristic of growth on these surfaces because, in each case, the epitaxial thickness was considerably smaller than the facet length.

ACKNOWLEDGMENTS

The authors appreciate the useful discussions with D. J. Eaglesham. This work is supported by NSF Contract No. DMR9202176.

[1] H. Sakaki, Jpn. J. Appl. Phys. **19**, L735 (1980).
[2] K. C. Rajkumar, A. Madhukar, K. Rammohan, D. H. Rich, P. Chen, and L. Chen. Appl. Phys. Lett. **63**, 2905 (1993).
[3] *Science and Engineering of One- and Zero-Dimensional Semiconductors*, edited by S. P. Beaumont and C. V. Sotomayor Torres (Plenum, New York, 1989).
[4] T. Yuasa, M. Mannoh, T. Yamada, S. Naritsuka, K. Shinozaki, and M. Ishii, J. Appl. Phys. **62**, 764 (1987).
[5] W. Q. Li and P. K. Bhattacharya, IEEE Electron. Device Lett. **EDL-12**, 385 (1991).
[6] H. P. Meier, E. Van Gieson, W. Walter, C. Harder, M. Krahl, and D. Bimberg, Appl. Phys. Lett. **54**, 433 (1989).
[7] J. S. Smith, P. L. Derry, S. Margalit, and A. Yariv, Appl. Phys. Lett. **47**, 712 (1985).
[8] M. Mannoh, T. Yuasa, S. Naritsuka, K. Shinozaki, and M. Ishii, Appl. Phys. Lett. **47**, 728 (1985).
[9] D. P. Adams and S. M. Yalisove, Mater. Res. Soc. Symp. Proc. **317**, 35 (1993).
[10] S. Guha and A. Madhukar, J. Appl. Phys. **73**, 8662 (1993).
[11] D. J. Eaglesham, G. Higashi, and M. Cerullo, Appl. Phys. Lett. **59**, 685 (1991).
[12] M. Lopez, T. Ishikawa, and Y. Nomura, Jpn. J. Appl. Phys. **32**, L1051 (1993).
[13] E. Kapon, M. C. Tamargo, and D. M. Hwang, Appl. Phys. Lett. **50**, 347 (1987).
[14] S. P. Murarka, in *Metallization: Theory and Practice for VLSI and ULSI* (Butterworth and Heinemann, Boston, 1993), p. 228.
[15] J. Aarts and P. K. Larsen, in *RHEED and Reflection Electron Imaging of Surfaces*, edited by P. I. Larsen and P. J. Dobson (Plenum, New York, 1988), p. 449.
[16] H. Jorke, H. J. Herzog, and H. Kibbel, Phys. Rev. B **40**, 2005 (1989).
[17] F. Jona, Appl. Phys. Lett. **9**, 235 (1966).
[18] D. J. Eaglesham, H.-J. Gossmann, and M. Cerullo, Phys. Rev. Lett. **65**, 1227 (1990).
[19] D. J. Eaglesham, F. C. Unterwald, G. S. Higashi, H. Luftman, D. P. Adams, and S. M. Yalisove, J. Appl. Phys. **74**, 6615 (1993).
[20] D. W. Pashley, in *Epitaxial Growth*, edited by J. W. Matthews (Academic, New York, 1975), Part A, p. 6.
[21] L. Bruck, Ann. Phys. (Leipzig) **26**, 233 (1936).
[22] D. P. Adams, S. M. Yalisove, and D. J. Eaglesham, Appl. Phys. Lett. **63**, 3571 (1993).
[23] M. Copel and R. M. Tromp, Phys. Rev. Lett. **72**, 1236 (1994).
[24] M. V. Ramana Murty, H. A. Atwater, A. J. Kellock, and J. E. E. Baglin, Appl. Phys. Lett. **62**, 2566 (1993).
[25] B. E. Weir, B. S. Freer, R. L. Headrick, D. J. Eaglesham, G. H. Gilmer, J. Bevk, and L. C. Feldman, Appl. Phys. Lett. **59**, 204 (1991).
[26] Y. W. Mo, J. Kleiner, M. B. Webb, and M. G. Lagally, Phys. Rev. Lett. **66**, 1998 (1991).
[27] C. C. Umbach, M. E. Keefe, and J. M. Blakely, J. Vac. Sci. Technol. A **9**, 1014 (1991).
[28] A. Ishizaka and Y. Shiraki, J. Electrochem. Soc. **133**, 66 (1986).
[29] S. M. Yalisove, D. P. Adams, and O. P. Karpenko (unpublished).
[30] S. Nikzad, S. S. Wong, C. C. Ahn, A. L. Smith, and H. A. Atwater, Appl. Phys. Lett. **63**, 1414 (1993).
[31] A thermocouple was used with an optical pyrometer to calibrate the substrate temperature for this setup.
[32] D. D. Perovic, G. C. Weatherly, P. J. Simpson, P. J. Schultz, T. E. Jackman, G. C. Aers, J. P. Noel, and D. C. Houghton, Phys. Rev. B **43**, 4257 (1991).
[33] Evidence of a crystalline-to-amorphous transition occuring during the growth of GaAs/GaAs(001) can be found in D. J. Eaglesham, L. N. Pfeiffer, K. W. West, D. R. Dykaar, and M. Cerullo, Appl. Phys. Lett. **58**, 65 (1991).
[34] Evidence of a crystalline-to-amorphous transition occuring during the growth of Ge/Si(001) can be found in D. J. Eaglesham and M. Cerullo, Appl. Phys. Lett. **58**, 2276 (1991).
[35] D. J. Eaglesham (private communication).
[36] B. Z. Olshanetsky and V. I. Mashanov, Surf. Sci. **111**, 414 (1981).
[37] D. J. Chadi, Phys. Rev. B **29**, 785 (1984).
[38] M. J. Hadley, S. P. Tear, B. Rottger, and H. Neddermeyer, Surf. Sci. **280**, 258 (1993).
[39] Y.-N. Yang, E. D. Williams, R. L. Park, N. C. Bartelt, and T. L. Einstein, Phys. Rev. Lett. **64**, 2410 (1990).
[40] W. Ranke, Phys. Rev. B **41**, 5243 (1990).
[41] J. Knall, J. B. Pethica, J. D. Todd, and J. H. Wilson, Phys. Rev. Lett. **66**, 1733 (1991).
[42] J. H. Wilson, P. D. Scott, J. B. Pethica, and J. Knall, J. Phys. Condens. Matter **3**, 5133 (1991).
[43] U. Myler and K. Jacobi, Surf. Sci. **220**, 353 (1989).
[44] H. Hirayama, M. Hiroi, and T. Ide, Phys. Rev. B **48**, 17 331 (1993).
[45] A. G. Dirks and H. J. Leamy, Thin Solid Films **47**, 219 (1977).
[46] H. E. Farnsworth, R. E. Schlier, and J. A. Dillon, Jr., J. Phys. Chem. Solids **8**, 116 (1959).